EGTRIB Journal
JOURNAL OF
THE EGYPTIAN SOCIETY OF TRIBOLOGY
VOLUME 19, No. 3, July 2022 pp. 20 - 35 **ISSN 2090 - 5882**
(Received June 03. 2022, Accepted in final form June 11. 2022) **jest.journals.ekb.eg**

DESIGN AND NUMERICAL ANALYSIS OF VERTICAL AXIS WIND TURBINE FOR ENERGY HARVESTING FROM HIGH-WAY VEHICLES MOTION

Nikhil Mandala[1], Mohamed Alkalla[1,2]

[1]Mechatronics Engineering and Intelligent Machines, School of Engineering, University of Central Lancashire, Preston, PR1 2HE, UK.
[2]On Leave; Production Engineering and Mechanical Design Dept., Mansoura University.

ABSTRACT
The rapid vehicles on the motorways (with speed ranging from 100 to 160 *Km/h*) cause excessive wind turbulence, which could be utilized to drive vertical axis wind turbines (VAWT), which in turn, can generate sufficient electrical power. VAWT is compact and represents an innovative solution for the narrow areas despite the horizontal axis turbines that require massive radial space and construction costs. By using an array of wind turbines on both sides of the highways, a significant amount of electricity will be generated which could be utilized for street lighting, electric car charging, and many other purposes. This article proposes a comparative study on the different parameters that could affect the VAWT performance. The CAD models of different VAWT designs are developed by CREO software, while the computational fluid dynamics (CFD) analysis is conducted by ANSYS software. The mechanical power generated by VAWT is calculated from the CFD analysis results and hence the electrical power is evaluated. The tribological study of the turbine aerodynamics by CFD concludes the performance of different blade heights and inclination angles with its rotor. It is noted that the generated power increases with increasing the blade height and inclination angle regression.

KEYWORDS
Vertical axis wind turbine, computational fluid dynamics, green energy, energy harvesting, urban regions.

INTRODUCTION
The power generation from conventional sources like fossil fuels (*e.g.*, natural gas, charcoal, petrol), from first glance, looks cheaper in terms of the amount of energy produced, cost of excavation, transportation ... etc. However, in the long term, it is very costly and dangerous due to its harmful emissions on human health and the entire planet's integrity. Therefore, green energy represents the future of the earth. Nowadays, it maintains sustainability, particularly, with the exponentially increasing human population and the excessive consumption of fossil fuels. Additionally, with the continuous rise in fossil fuel prices worldwide, power generation from conventional sources is no longer cheap [1]. On the

opposite hand, most of the wind power cost is contributed to the establishment of wind turbines, because the fuel—the breeze—is free, [2]. Once they were established, no running costs except maintenance are required. The data from the Wall Street Journal, shown in Fig. 1, illustrates that the cost of power generation (*$/MW*) from wind farms is nearly the same as power generation from natural gas power plants [2]. Also, the power generation from wind farms can be increased by increasing the rotor diameter of the horizontal axis wind turbine (HAWT). This power ranges from 50 *kW* to 5 *MW* for a rotor diameter of 15 *m* to 112 *m*, respectively, [1].

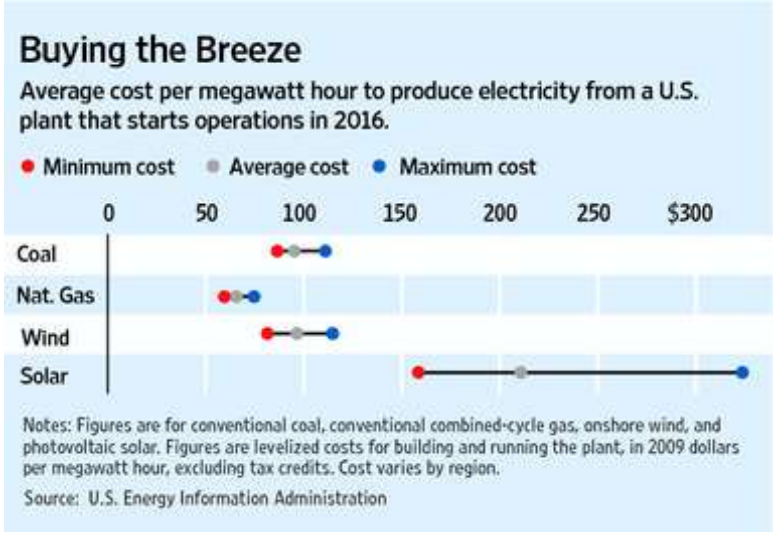

Fig. 1 Power projection from new plants in 2016, [2].

A review study, accomplished by Ahmed and Cameron, [3], on the latest wind power technologies shows that greater public awareness has been seen in the recent years about the significance of wind power as a sustainable source, the issues regarding noise, land use, avian deaths, electromagnetic interference, and visual effects must be resolved to ensure continued public and political support for the acceptance of HAWTs. Although there are more consistent winds at rural sites compared to urban, as discussed in a study achieved by Sunderland et al., [4] in Ireland, Sri Lanka, and the UK, there is also higher wind turbulence due to the uneven topologies of the urban areas which can accommodate VAWT easily instead of the traditional huge wind farms. Hence, in such regions, energy harvesting systems such as highway VAWT are the optimum solution. Early development of VAWT started in the 1980s and many predictive studies reveal that the installation cost and performance of VAWT would be more effective shortly with the increasing demands on energy generation, [5].

VAWT is the best choice for applications involving low power requirements like street lighting, telecommunication, charging points, … *etc*. VAWT can be placed on either side of highways and transforms the airflow generated from moving vehicles into useful electrical power. The statistical analysis carried out by various researchers has shown that the wind speed produced by moving vehicles is nearly 24 *m/s* (~86 *km/h*) and the speed at which it hits the wind turbine blades is at least 5 *m/s*, [6]. It shows that the best height to locate the VAWT blades is 3.3 *m* for the cars and 5.5 *m* for the buses and long vehicles.

Okubo et al., [7] demonstrated the effect of the vehicle passing by VAWTs and that they are generating a wind speed of 25 *m/s* and a power of 1 *kW*. A review conducted by Prajapati et al., [8] investigated both vertical and horizontal axis wind turbines. The horizontal type of windmill is preferable for large-scale applications and when sufficient space is available, if the space is limited then VAWT is preferable. It has the advantage of producing electricity at a low cost for domestic purposes and could be used to drive home appliances with low power, as investigated by Hossain et al., [9]. The experimental tests of this study were conducted at different air velocities (*i.e., 20 m/s and 25 m/s*). The power generated at 20 *m/s* air speed was 567 *W*, while at 25 *m/s* is 709 *W*.

Another advantage of VAWT is its self-starting characteristic despite HAWT that needs a special starting system and is not feasible in the urban regions where the intensity of wind is lower than in vast open areas, [10]. This study also showed that a combination of Savonius turbine and NACA0030 airfoil can easily represent a self-start mechanism for VAWT. In addition, Batista et al., [11], proposed a new blade profile (*i.e.* EN0005) and it has been operated efficiently at a low air-speed of 1.25m/s and has a self-starting feature, also this wind turbine prototype exhibited good stability at higher wind speeds (*i.e.* 25m/s). A further study conducted by Varun et al., [12] revealed that combined (Savonius+Darrieus) rotor VAWT has higher efficiency than the single Savonius or Darrieus rotor, and it has been emphasised by Asadi and Hassanzadeh, [13]. Figure 2 illustrates simplified designs of different wind turbine types and different configurations, [14], [15].

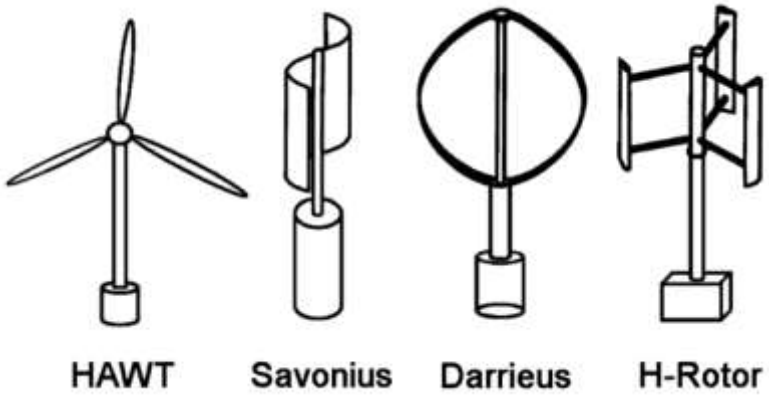

Fig. 2 Different types of the wind turbine, [15].

The numerical analysis tools are powerful in broadcasting, investigating, and evaluating the performance of the proposed designs before the fabrication phase. A numerical investigation on small scale Darrieus turbine has been performed by Howell et al., [16], CFD results have a close agreement with experimental results performed through that study with an error of 20% observed for coefficient of power (Cp) and tip speed ratio (TSR). In a comparison between Darrieus and Savonius turbines, the Darrieus turbine has better aerodynamic performance compared to the Savonius turbine, [17]. The Darrieus turbine working principle is based on aerodynamic lift force and it extracts more energy from the swept area of the turbine blade. Two and three-bladed hybrid Darrieus-Savonius turbines introduced in [18] and [19], respectively, showed that their power coefficient is higher (ranging from 0.18 and 0.53) compared to Savonius rotor (ranging from 0.15 to 0.38). Therefore, a hybrid Darrieus-Savonius could be a better option for domestic places having less space and where

wind speed is also low. Few works focused on the H-Rotor VAWT type such as; Peng et. al., [20], Lositaño and Danao, [21], and Mohamed, M.H. [22]. Hence, the scope of this study will concentrate on this type based on different parametric designs and its feasibility to generate power from the vehicle motion. The effect of VAWT blade height and inclination angle of the blade with the rotor on the power generation is investigated using CFD. The numerical model on CFD simulation of VAWT operating at low and high external air speeds is also presented. The numerical model can be used for further analysis of VAWT with any other design configuration.

VAWT DESIGN AND RESEARCH METHODOLOGY

This section presents the methodology of the conducted study as depicted in the schematic diagram in Fig. 3. Mainly the study depends on numerical investigation of VAWT using ANSYS CFX.

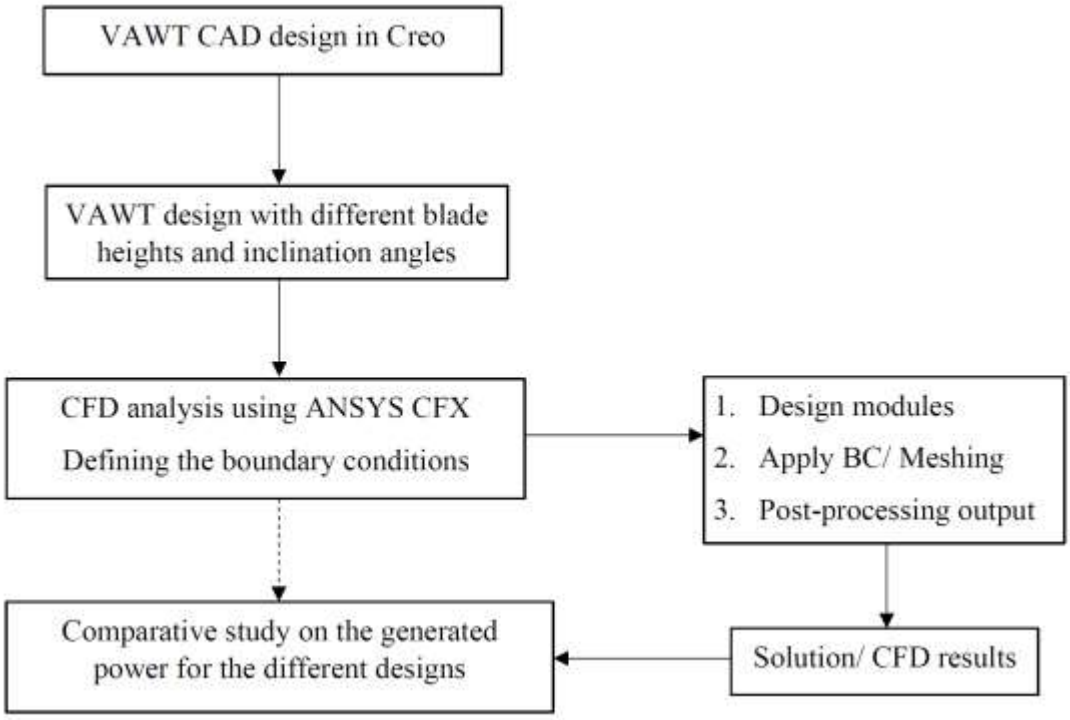

Fig. 3 Schematic diagram of the proposed study.

The airfoil of NACA 0012 is designed using 3D Creo CAD software for the wind turbine, this airfoil is used to construct the turbine blades, as shown in Fig. 4. The airfoil is designed with different heights which are 400, 600, and 800 *mm*. These blades are assembled with base structure and top plate structure to form a complete VAWT assembly with a rotor diameter of 562 *mm*, as shown in Fig. 5. Three bladed VAWT is selected based on a study achieved by Roy and Saha, [23], which showed that the drag force can be reduced by varying the number of blades, and blade orientation angles. They mentioned that "variation in the blade numbers influence the *Cp*, and the best performance was accomplished with three blades".

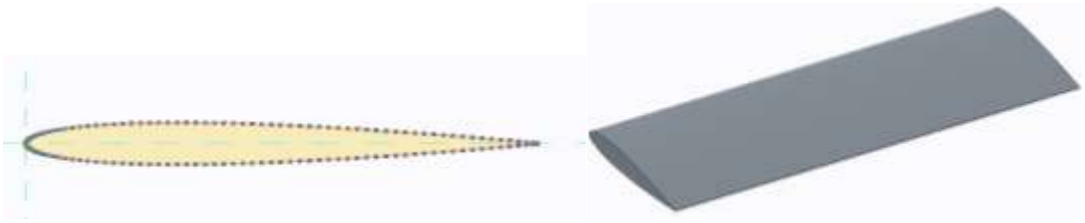

(a) **(b)**

Fig. 4 NACA 0012 air foil design (a) profile sketch and (a) extrusion feature

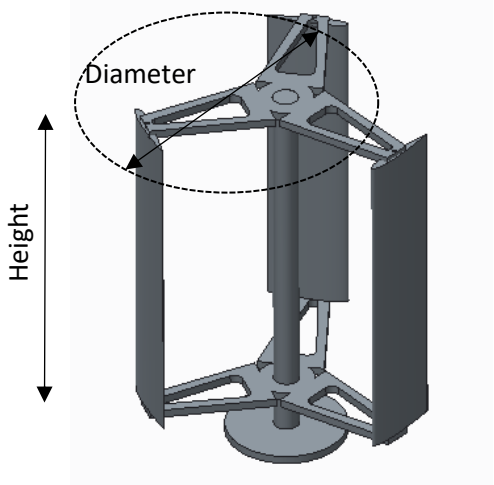

Fig. 5 VAWT with 400 *mm* turbine height.

The VAWT CAD design is exported to ANSYS, and the computational domain needs to be defined for further analysis. For this purpose, a zone surrounding the VAWT assembly is generated to model the wind flow. The dimensions of this zone are 0.9*m* ×0.9*m*×0.9*m*, as shown in Fig. 6. The thermodynamic properties of the air at 25^{o}C are defined as; Molar mass is 28.96 *g/mol*, density is 1.185 kg/m^3, specific heat capacity is 1004.4 *J/(kg.K)*, and reference pressure is 1 *atm*. The material of the turbine is selected as Aluminium with the following properties; a Molar mass of 26.98 *g/mol*, a density of 2702 kg/m^3, and a specific heat capacity of 903 *J/(kg.K)*. As the VAWT model doesn't have topological consistency and is complex, so, brick meshing is not feasible. Therefore, the entire domain is meshed using a tetrahedral element type, as illustrated in Fig. 7. The sizing is set to fine and the curvature size function is set. The number of generated nodes is 4154966 and the number of elements is 789244.

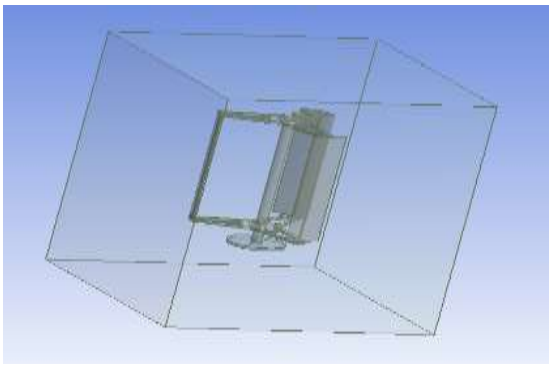

Fig. 6 Imported VAWT assembly and definition of simulation domain in ANSYS.

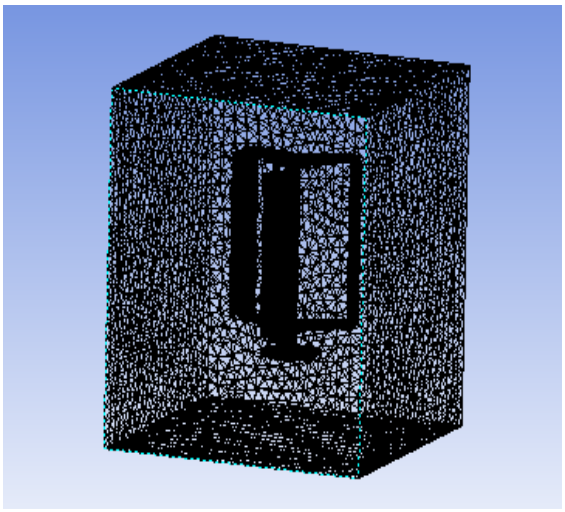

Fig. 7 Wireframe meshed model of the turbine and surrounding domain.

The domain definition is made for the surrounding zone of VAWT. The domain type is set to fluid and the material is air. The reference pressure is set to 1 *atm* with a k-epsilon turbulence model. This model is relatively simple, and the computation time is less. It belongs to the Reynolds-averaged Navier Stokes (RANS) family of turbulence models where all the effects of turbulence are modelled. The blade is defined as a solid domain type. The air inlet boundary conditions, shown in Fig. 8, are defined at 5 *m/s* and 10 *m/s*, respectively. The air outlet boundary condition is defined with 0 relative pressure differences.

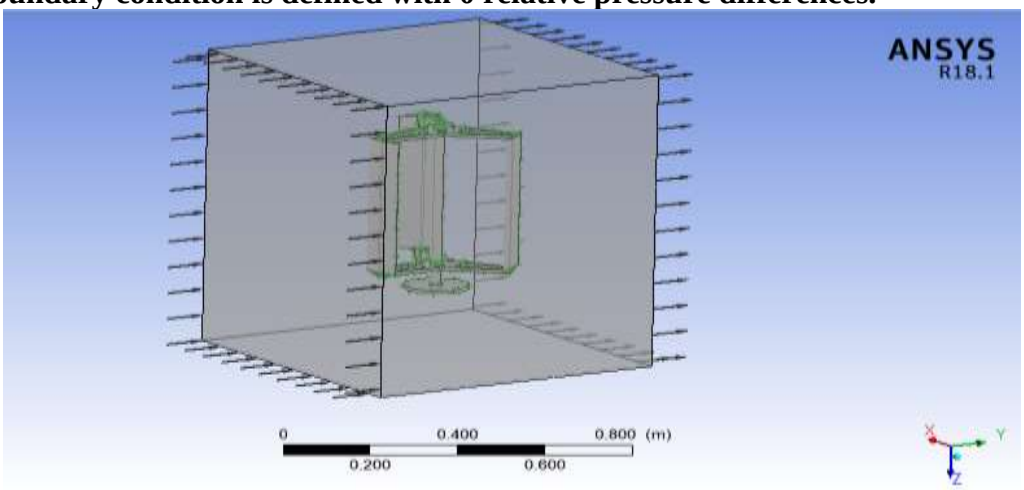

Fig. 8 Boundary condition of CFD model.

The interface is defined between VAWT solid domain and the outside air-fluid domain. The interface defined is of general grid interface (GGI) type where multiple grids with faces that touch each other can be handled. GGI connections permit non-matching of node location, element type, surface extent, surface shape, and even non-matching of the flow physics across the connection. The solver settings are defined for CFD simulation to include setting up RMS residual target values and the maximum number of iterations. The RMS residual target is set to 0.0001 whereas the total number of iterations is set to 200, as shown in Fig. 9 and 10.

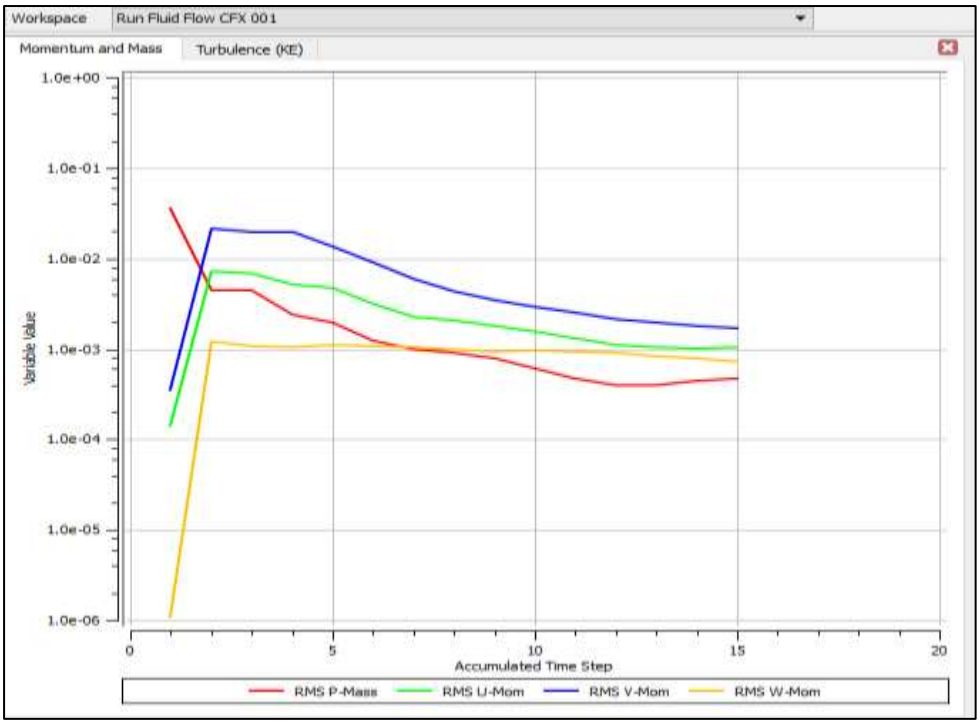

Fig. 9. Momentum and mass RMS residual plots.

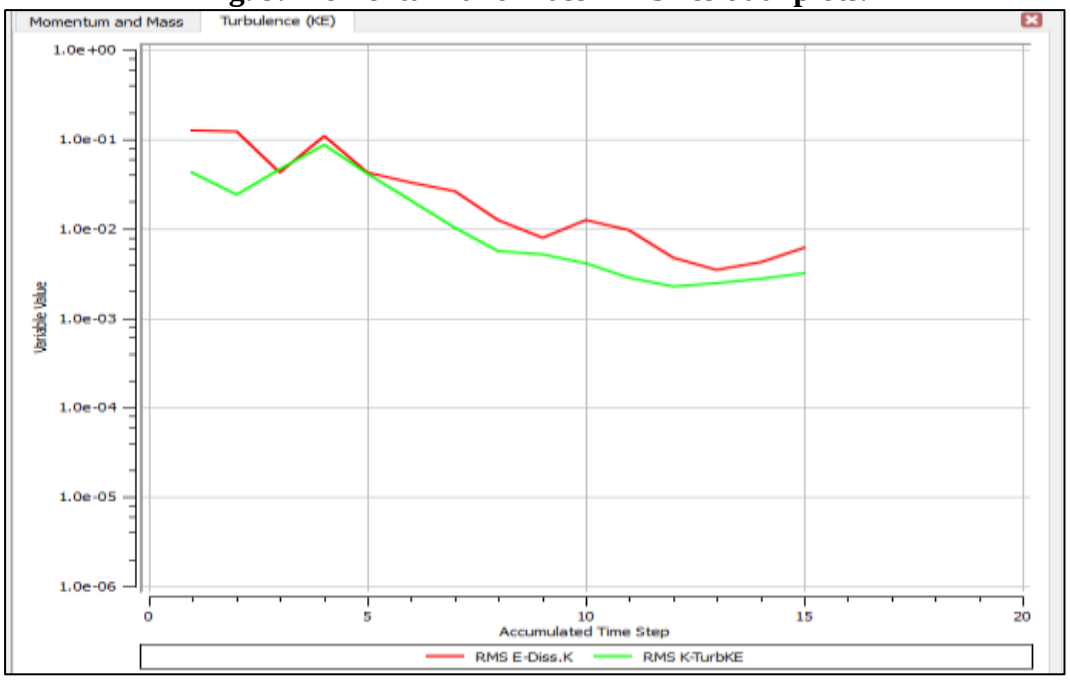

Fig. 10 Turbulence kinetic energy RMS residual plots.

NUMERICAL SIMULATION RESULTS

CFD is mainly used for flow field visualisation of the proposed VAWT designs. Firstly, The CFD analysis results are generated for VAWT with different blade heights. The different design configurations are 400, 600, and 800-*mm* turbine height at a fixed inclination angle of the blades with the rotor equal to 0^{o}. The inclination angle for turbine blades to be analysed are 20^{0}, $30^{0,}$ and 40^{0}, they are going to be studied later at a fixed blade height of 800 *mm*. As

mentioned/discussed by multiple research works, the average wind speed that hits the turbine blades is at least 5 *m/s*, [6]. Indeed, this vehicle wind flow will be backed by the natural wind stream crossing over the highways too. So, a speed of 5 *m/s* is considered here as the minimum wind velocity in addition to another higher speed of 10 *m/s* for all varying parameters through the current study.

EFFECT OF BLADE HEIGHT

1. Wind Turbine Height 400mm

Initially, the CFD analysis is conducted for 400mm-height VAWT at 5 *m/s* inlet wind velocity. The velocity contour plots on the blade surfaces are generated, as shown in Fig. 11. It is noted that maximum velocity is observed at the blade tips with a magnitude of more than 9.073 *m/s*, whereas the mid-region of blades has a lower velocity of 0.012 *m/s*. The pressure plot is generated for this design as well, as shown in Fig. 12. It shows that the maximum pressure occurs at the blade profile tail with a value of 23.29 *Pa*, while the minimum occurs at the frontal face of the blade profile with a value of -94.7 *Pa*.

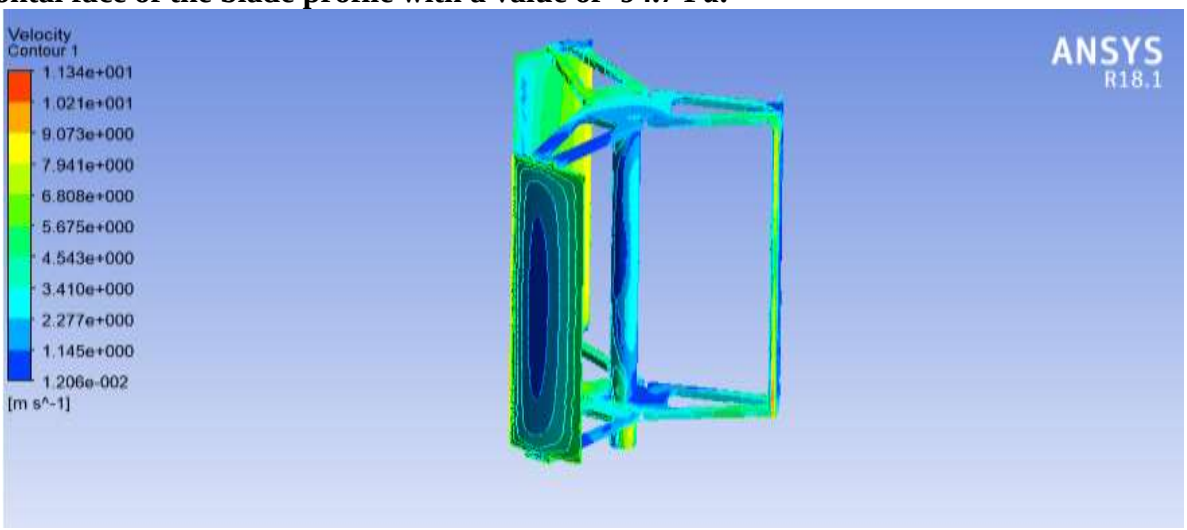

Fig. 11 Velocity contours at 5*m/s* inlet wind velocity for 400*mm*-height VAWT.

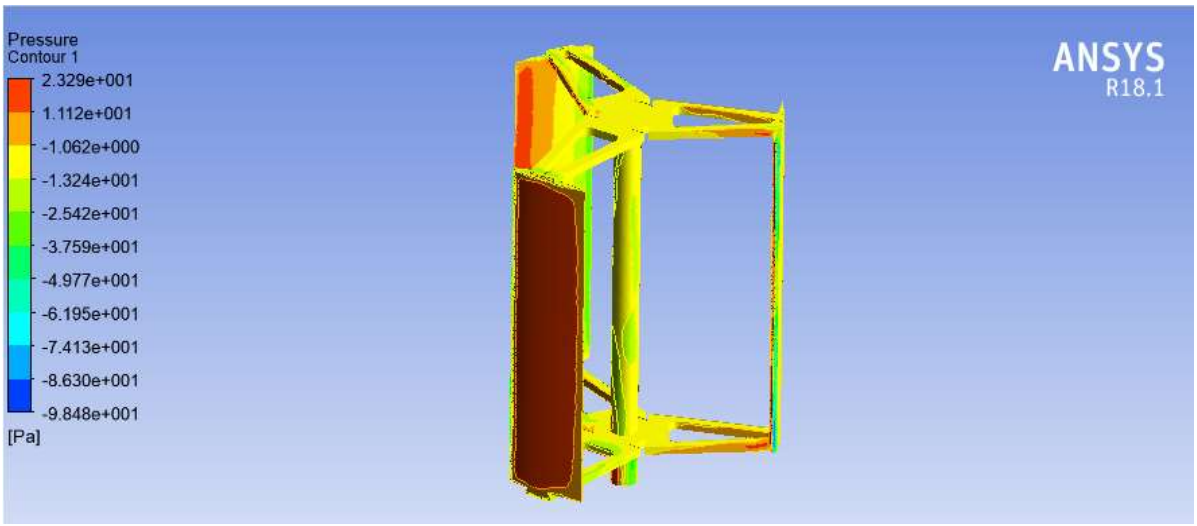

Fig. 12 Pressure contours at 5*m/s* inlet wind velocity for 400*mm*-height VAWT.

At 10 *m/s* inlet wind velocity, similarly, the CFD analysis resulted in velocity vectors and pressure contours on the blade surfaces and they are plotted in Fig. 13 and 14, respectively. The plots illustrate that the maximum velocity vectors exerted are at the blade tips with a magnitude of 27.1 *m/s*, whereas, the mid-region of blades has a lower velocity of less than 6.77 *m/s*. Furthermore, the maximum pressure is observed also at the blade tail with a maximum value of 91.25 *Pa*, whereas the lowest is at the front face with a value of -500.6 *Pa*.

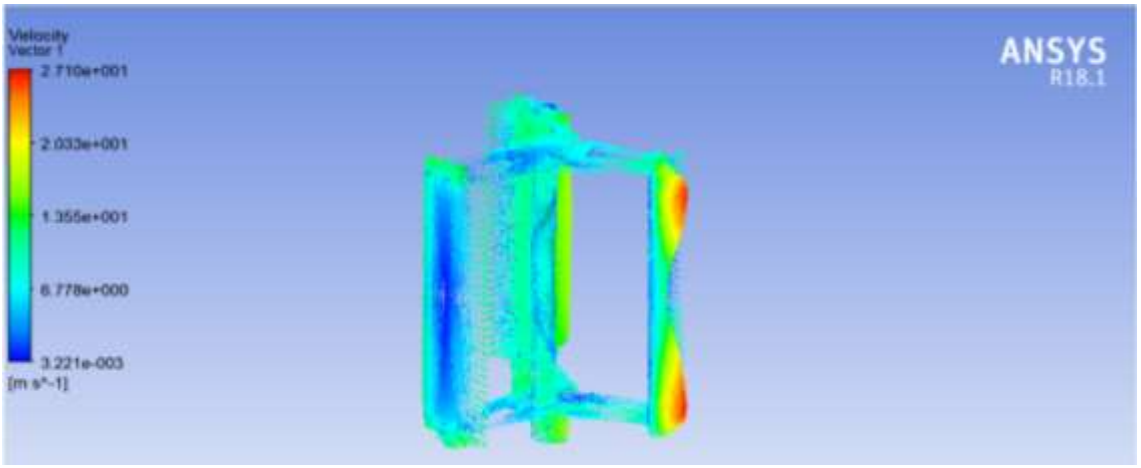

Fig. 13 Velocity vectors at 10*m/s* inlet wind velocity for 400*mm*-height VAWT.

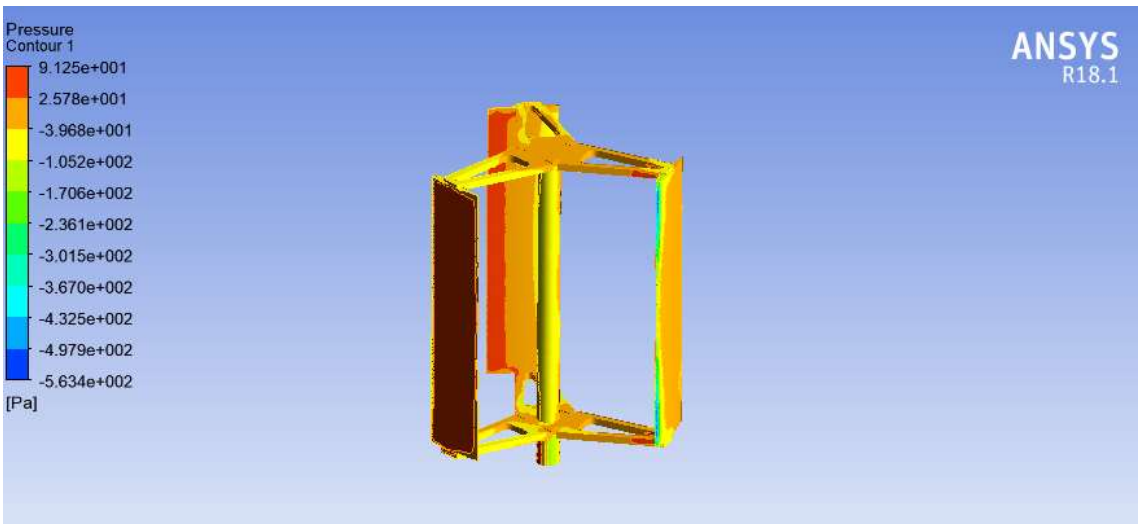

Fig. 14 Pressure contour at 10*m/s* inlet wind velocity for 400*mm*-height VAWT.

2. Wind Turbine Height 600 mm

The same aforementioned analysis has been conducted for the 600*mm*-height VAWT enclosed with a wind of 5 *m/s* and 10 *m/s* velocities. The CFD analysis at 5 *m/s* studied both the velocity and pressure contours on the blades. It shows that maximum velocity is observed also at the blade tips with a magnitude of 13.4 *m/s*, while the mid-region of blades has the lowest velocity of 0.0128 *m/s*. Accordingly, the maximum pressure value is measured at the blade profile tail (*i.e.*, 25.1 *Pa*) and the minimum is at the frontal face of the blade (*i.e.*, -146 *Pa*).

Similarly, at the wind velocity of 10 *m/s*, it is evident that maximum velocity is observed at the blade tips with a magnitude of 28.3 *m/s*. The blade tip has maximum velocity whereas also the mid-region of blades has a lower velocity of 2.85 *m/s*. The pressure plot is generated also at the same wind velocity (*i.e.*, 10 *m/s*). The pressure is observed to be maximum at the blade profile tail with a value of 99.8 *Pa* and minimum at the frontal face of the blade with a value of -642.2 *Pa*.

3. Wind Turbine Height 800 mm

The CFD analysis is also conducted for blade height of 800 *mm*. The velocity contour plots are generated, as shown in Fig. 15. Although the velocity vectors look evenly distributed on the blades, the maximum velocity is still observed at the blade tips with a magnitude of 13.47 *m/s*. The blade tip has maximum velocity whereas, the mid-region of blades has the lowest velocity of 0.0073 *m/s*. The pressure plot in Fig. 16 displays the maximum pressure of 26.7 *Pa* occurring at the blade profile tail and while the minimum value of -148.1 *Pa* occurs at the frontal face of the blade.

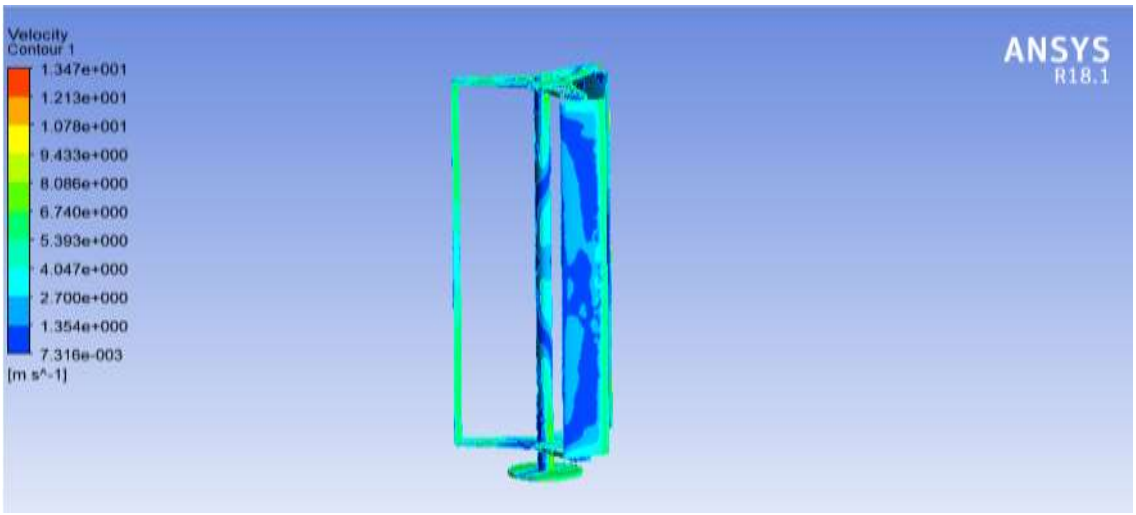

Fig. 15 Velocity contours at 5*m/s* inlet wind velocity for 800*mm*-height VAWT.

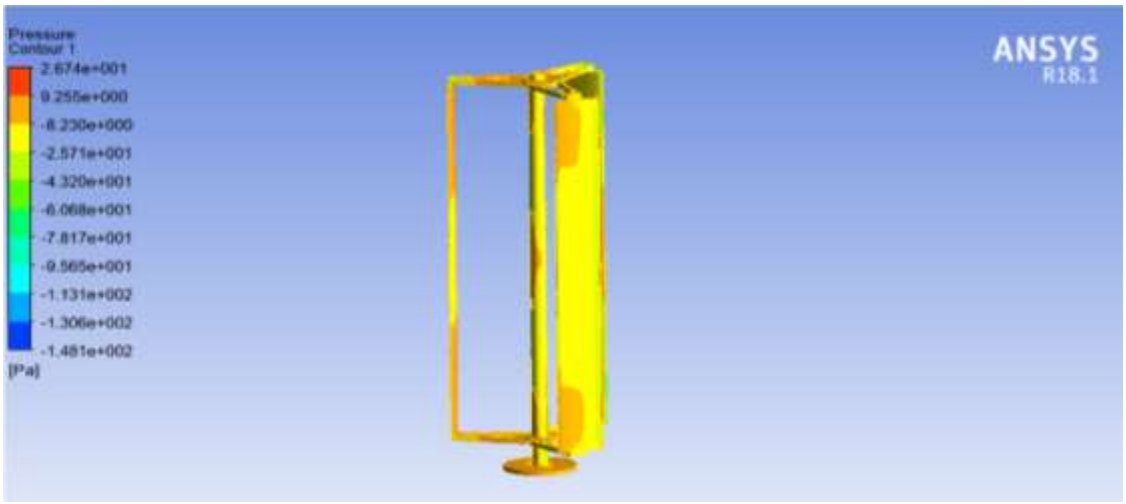

Fig. 16 Pressure contour at 5m/s inlet wind velocity for 800mm-height VAWT.

The same analysis has been applied at the higher wind velocity (*i.e.*, 10 m/s), and the CFD analysis shows the same trend for the blade surfaces velocity and pressure. The blade tip has a maximum velocity of 28.7 *m/s*, whereas the mid-region of blades has the lowest velocity of 0.0071 *m/s*. Likewise, the pressure is observed to have a maximum of 106.5 *Pa* at the blade profile tail and a minimum of -645.3 *Pa* at the frontal face. Figures 17 and 18 illustrate the velocity and pressure on the blade surfaces for the three different turbine heights.

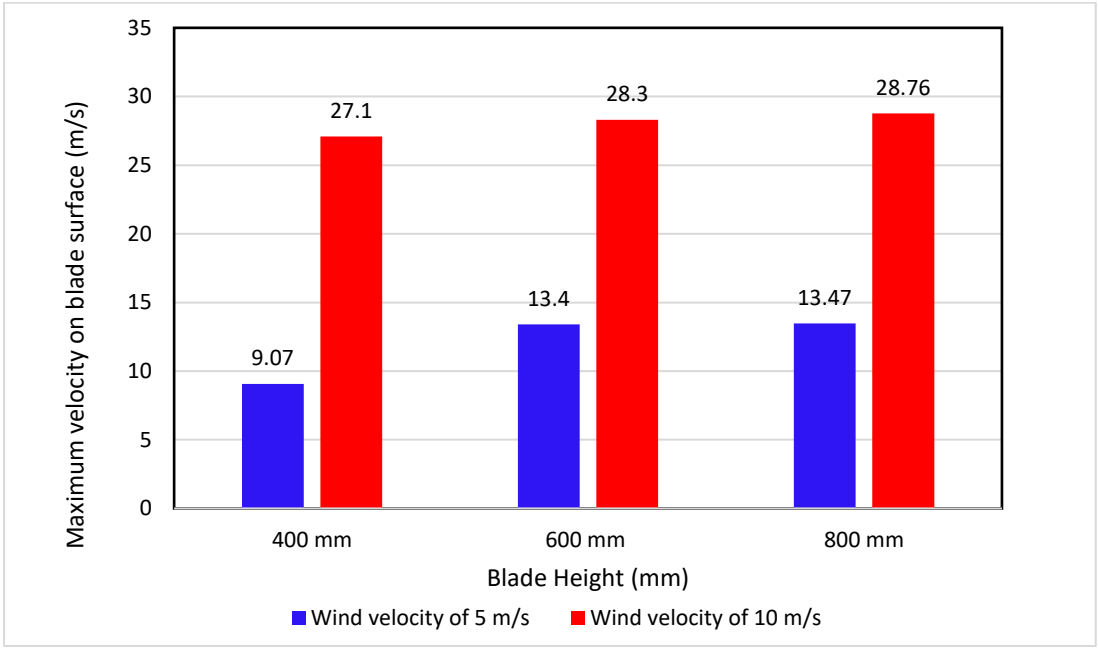

Fig. 17 The maximum velocity on the blade surface for different blade heights and wind velocities.

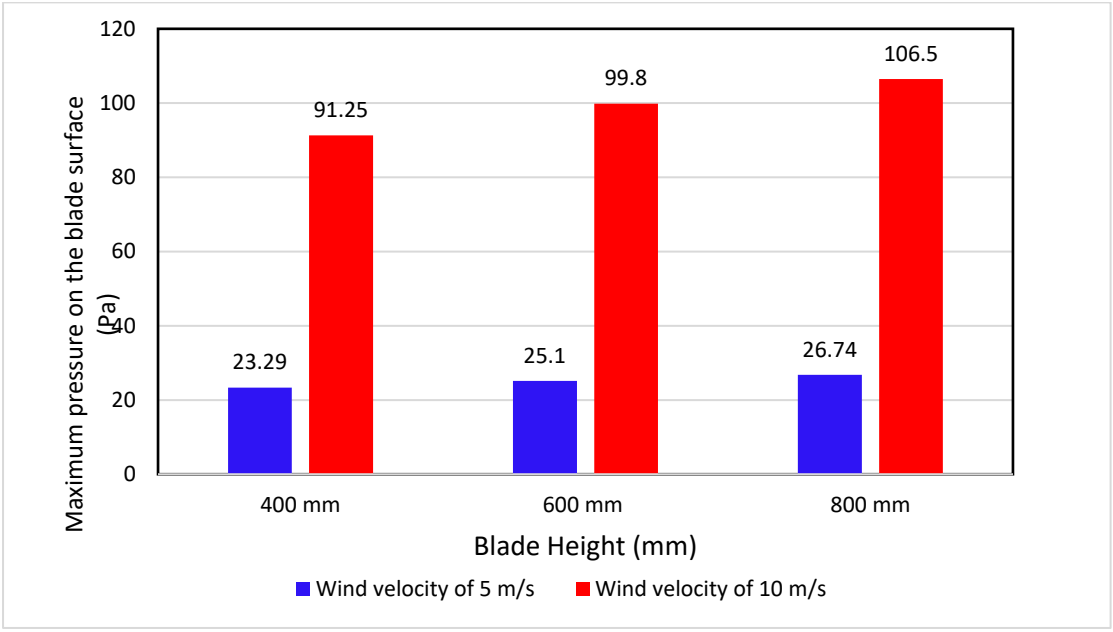

Fig. 18 The maximum pressure on the blade surface for different blade heights and wind velocities.

EFFECT OF BLADE INCLINATION ANGLE

The effect of different inclination angles (ϕ) of the VAWT blades with the rotor is studied in this section. The CFD analysis is conducted for 800mm-height VAWT with different blade inclination angles of 20º, 30º, and 40º, as shown in Fig. 19. The study considers the change in the blade inclination angle *w.r.t* the rotor while keeping a fixed direction of the wind. This is because the moving vehicles normally have a fixed linear displacement on the roads in only one direction. The analysis has been performed for the predefined wind velocities (*i.e.*, 5 and 10 *m/s*). Figures 20 and 21 summarised the resultant maximum velocities and pressures on the blade surfaces.

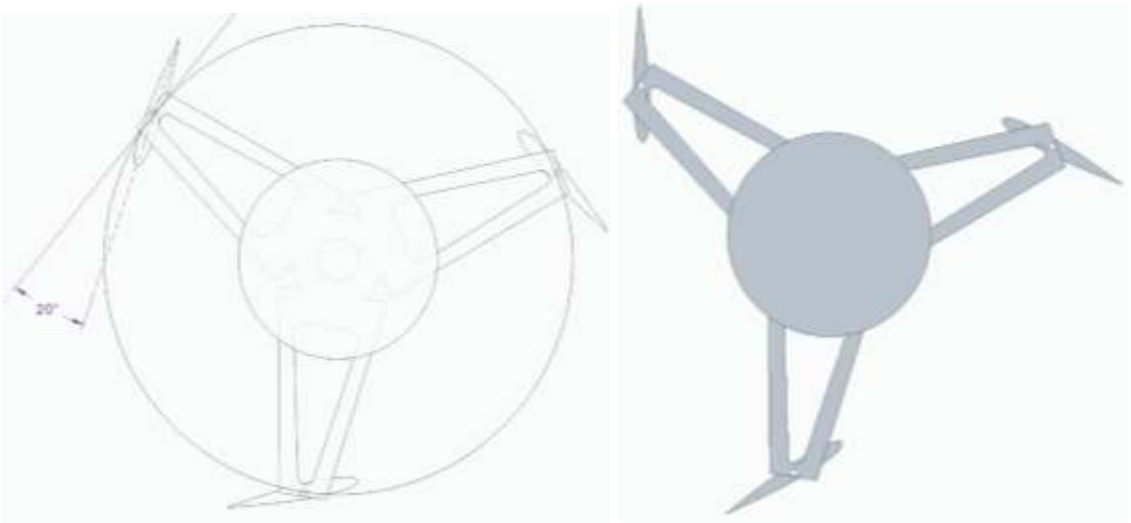

(a) ϕ= 20º **(b) ϕ= 40º**

Fig. 19. Three-Bladed H-Rotor VAWT configuration and blade inclination angle.

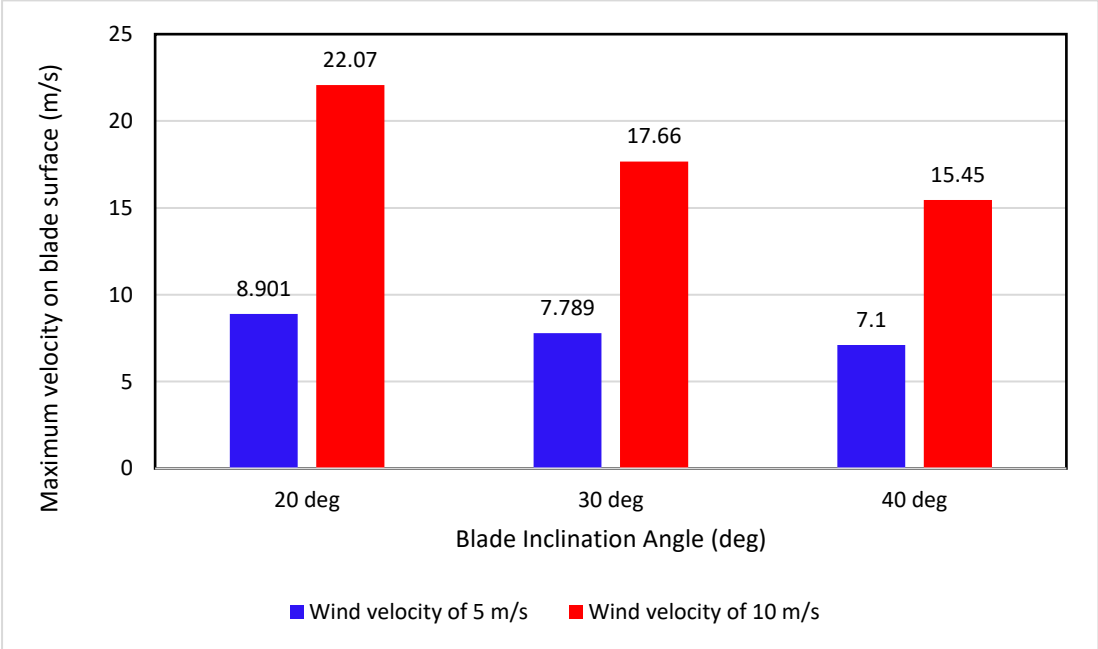

Fig. 20 Maximum velocity on the blade surface for different inclination angles and wind velocities.

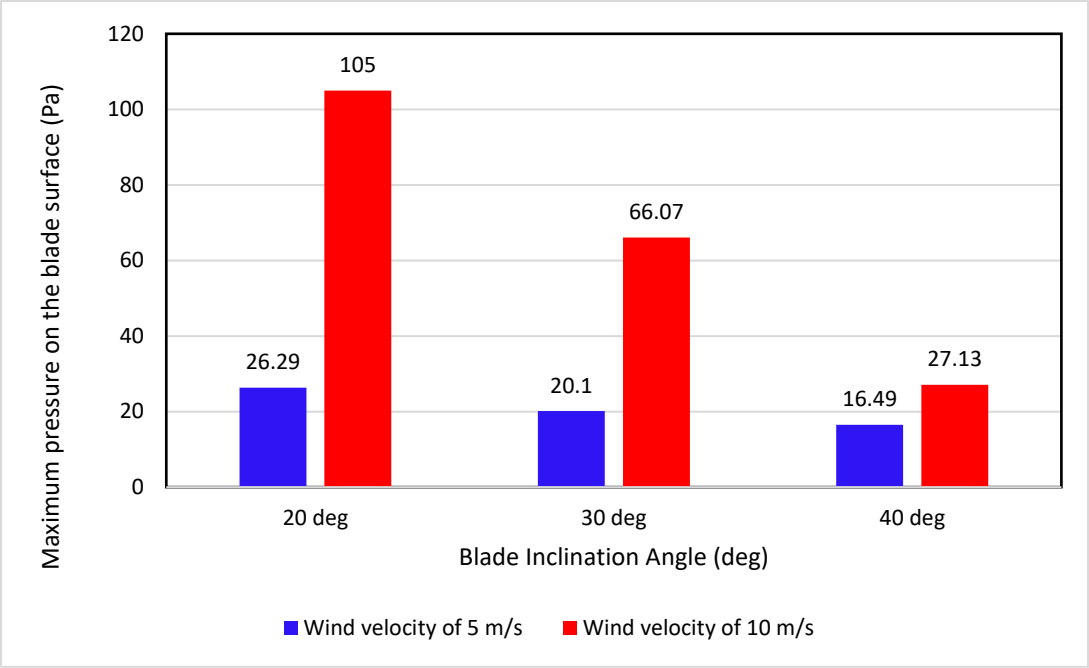

Fig. 21 Maximum torque on the turbine rotor for different inclination angles and wind velocities.

DISCUSSION

The electric power can be calculated and predicted based on the CFD analysis conducted in the previous section to determine the effect of the blade height and inclination angle. The aggregated power will be utilised to energise useful applications on the highways such as; electric car charging stations, night-lightening of the roads, telecommunications tower energising, and billboard lighting. As the electric power collected by the generators from the turbine has a relation with the mechanical power from the physical motion of rotor angular displacement. Therefore, the following relationship applies:

$$P_e = \eta\, P_m$$

where P_e is the electrical output power, η is the efficiency coefficient which is dependent on multiple factors such as the friction between the turbine rotor and its bearings, friction between the generator rotor (armature) and its bearings, both mass and inertia of the turbine and generator rotors, …etc. It is recommended by Sunny and Kumar to consider a coefficient of efficiency of 70% for transformation from mechanical to electrical power, [24]. P_m is the mechanical power calculated on the turbine rotor due to the wind flow and expressed as, [22], [25]:

$$P_m = 0.5\, C_p \rho A_s V^3$$

Where, C_p is the coefficient of power, according to Albert Betz, no wind turbine can convert the kinetic energy of the wind to mechanical energy of more than 59.3%, [26], ρ is the air density, A_s is the total blade surface area, and V is the wind velocity on the blade. The mechanical and electrical power for different blade heights and inclination angles are calculated at 5 *m/s* and 10 *m/s* inlet air speed and presented in Table. 1 and 2, respectively.

Table.1 Mechanical and electrical power at different blade heights of VAWT

Turbine		5 *m/s* wind velocity			10 *m/s* wind velocity		
Blade Height	Surface area, $A_{s\ (3blades)}$ (m^2)	V_{blade} (m/s)	P_m (watt)	P_e (watt)	V_{blade} (m/s)	P_m (watt)	P_e (watt)
400 *mm*	0.0895	9.07	23.345	16.341	27.1	622.689	435.882
600 *mm*	0.1335	13.4	112.289	78.602	28.3	1057.745	740.421
800 *mm*	0.1775	13.47	151.650	106.155	28.76	1476.065	1033.245

Table. 2 Mechanical and electrical power at different blade inclination angles of VAWT

Turbine		5 *m/s* wind velocity			10 *m/s* wind velocity		
Blade angle ϕ	Surface area, $A_{s\ (3blades)}$ (m^2)	V_{blade} (m/s)	P_m (watt)	P_e (watt)	V_{blade} (m/s)	P_m (watt)	P_e (watt)
20^o	0.1775	8.901	43.758	30.630	22.07	667.031	466.921
30^o	0.1775	7.789	29.321	20.525	17.66	341.752	239.226
40^o	0.1775	7.10	22.208	15.546	15.45	228.836	160.185

The results show that increasing the blade height increases the generated power. The maximum power generated at 10 *m/s* is 1.03 *kW* which is very efficient for charging or operating small appliances. The effect of blade inclination angle on power generation is given in Table 2. The research findings have shown that the power decreases with increasing inclination angle ϕ with the rotor. The optimum inclination angle should be very close to zero. As a comparison for different blade inclination angles the maximum power is observed between 0^0 to 20^0. The materials of VAWT affect its strength against storms and it requires further investigation, especially at high rotational speeds. Hence wear-resistant materials are required to increase the blades life. The future work will include studying the effect of topology optimization of the blade structure on the applied velocity of the blades and rotor torque, hence generating higher power. The proposed optimization algorithms include the method of moving asymptotes (MMA) based on a comparative study between different algorithms and their efficiency, [27]. The application of lightweight composite material for VAWT will be tested too.

CONCLUSIONS

The paper studied the effect of the parametric design of the blade geometry (i.e., height) and configuration (blade inclination angle ϕ) on the generated power. The advantages of running at lower wind speeds, the ability to operate in any wind flow direction, compact construction, and quietness make VAWT the ideal solution for power generation on the highways. Sustainability is maintained by such creative ideas of generating renewable and green energy. This makes the planet breathe easily again and reduces carbon monoxide and dioxide emissions and global warming.

The performance of the VAWT turbine has been evaluated using the CFD analysis. It significantly reduces the time and cost required for the evaluation of VAWT performance subjected to varying operation conditions. The CFD results have shown that the pressure

field and velocity field change with the rotation of the turbine blade. The difference in pressure across the VAWT blade generates lift force which rotates the turbine. The study recommends that increasing the blade's height and decreasing the inclination angle both increase the generated electrical energy. The critical regions of high pressure and low pressure across VAWT blades are determined which may need special reinforcement in the fabrication process and inspection precautions.

The current study would encourage the usage of VAWT (coupled with generators and batteries) as an alternate energy source and energy storage system in small applications, while fully connected with the electricity grid for large-scale energy feed. The energy generated from VAWT could be utilized in electric car charging points, night-lightening of the roads, telecommunications tower energising, mobile charging points, and Billboard lighting. Furthermore, the application of VAWT on top of vehicles and house roofs requires thorough investigation in a future study.

REFERENCES

1. McGowan J. G., and Connors S. R., "WINDPOWER: A Turn of the Century Review", Annual Review of Energy and the Environment, 25:1, pp. 147 - 197, (2000), https://doi.org/10.1146/annurev.energy.25.1.147

2. Ball J., "Wind Power Hits a Trough", Wall Street Journal, (2011, April 11).

3. Ahmed N. and Cameron M., "The challenges and possible solutions of horizontal axis wind turbines as a clean energy solution for the future", Renewable and Sustainable Energy Reviews, 38, pp. 439 - 460, (2014).

4. Sunderland K., Narayana M., Putrus G., Conlon M. and McDonald S., "The cost of energy associated with micro wind generation: International case studies of rural and urban installations" Energy, 109, pp. 818 - 829, (2016).

5. Islam M. R., Mekhilef S., and Saidur R., "Progress and recent trends of wind energy technology", Renewable and Sustainable Energy Reviews, Vol. 21, pp. 456 - 468, (2013).

6. Hegde. S. S., Thamban A., Bhai S. P. M., Ahmed A., Upadhyay M., Joishy A. and Mahalingam A. "Highway Mounted Horizontal Axial Flow Turbines for Wind Energy Harvesting from Cruising Vehicles." Proceedings of the ASME 2016 International Mechanical Engineering Congress and Exposition. Volume 6B: Energy. Phoenix, Arizona, USA. November 11–17, (2016). https: //doi.org/ 10.1115/ IMECE2016-65194

7. Okubo H., Hatakeyama R., Onodera H., Sato T., Fujii H., Maruyama Y. and Iwahara M., "Airborne Wind Power Generation Using a Straight Wing Vertical Axis Wind Turbine", The Proceedings of Conference of Kanto Branch, 2019.25(0), pp. 18E16, (2019).

8. Prajapati G. M., Abrarkhan I. P. and Patel M. B., "A Review: Aerodynamic Analysis on Vertical Axis Wind Turbine Blade", International Journal of Advance Engineering and Research Development, 1(12), (2014).

9. Hossain A., Iqbal A. K. M. P., Ataur R., Arifin M., and Mazian M., "Design and Development of A 1/3 Scale Vertical Axis Wind Turbine for Electrical Power Generation", Journal of Urban and Environmental Engineering 1, No. 2: pp. 53 - 60, (2007).

10. Abid M., Khasan S. K., Hafiz A-W, Furqan F., Hamza A. and Osama H. K., "Design, Development and Testing of a Combined Savonius and Darrieus Vertical Axis Wind Turbine", iranica journal of energy and environment 6(1), (2015).

11. Batista N., Melício R., Mendes V., Calderón M. and Ramiro A., "On a self-start Darrieus wind turbine: Blade design and field tests", Renewable and Sustainable Energy Reviews, 52, pp. 508 - 522, (2015).
12. Varun A., "A review of vertical axis wind turbine", Asian Journal of Multidimensional Research, 10 (11), pp. 654 - 660, (2021).
13. Asadi, M. and Hassanzadeh, R., "Effects of internal rotor parameters on the performance of a two bladed Darrieus-two bladed Savonius hybrid wind turbine", Energy Conversion and Management, 238, p. 114109, (2021).
14. Aslam Bhutta M., Hayat N., Farooq A., Ali Z., Jamil S. and Hussain Z., "Vertical axis wind turbine – A review of various configurations and design techniques", Renewable and Sustainable Energy Reviews, 16(4), pp. 1926 - 1939, (2012).
15. Mehrpooya P., "Improvement of vertical-axis wind turbine performance via turbine coupling", PhD diss., Illinois Institute of Technology, (2014).
16. Howell R., Qin N., Edwards J. and Durrani N., "Wind tunnel and numerical study of a small vertical axis wind turbine" Renewable Energy, 35 (2), pp. 412 - 422, (2010).
17. Jin X., Zhao G., Gao K. and Ju W., "Darrieus vertical axis wind turbine: Basic research methods", Renewable and Sustainable Energy Reviews, 42, pp. 212 - 225, (2015).
18. Ghosh A., Biswas A., Sharma K. and Gupta R., "Computational analysis of flow physics of a combined three bladed Darrieus Savonius wind rotor", Journal of the Energy Institute, 88 (4), pp. 425 - 437, (2015).
19. Roy S. and Saha U., "Wind tunnel experiments of a newly developed two-bladed Savonius-style wind turbine", Applied Energy, 137, pp. 117 - 125, (2015).
20. Peng H. Y., Liu, H. J., Yang, J. H., "A review on the wake aerodynamics of H-rotor vertical axis wind turbines", Energy, Volume 232, ISSN 0360-5442, (2021). https: //doi.org /10.1016/j.energy.2021.121003.
21. Lositaño I. C. M. and Danao, L. A. M., "Steady wind performance of a 5 kW three-bladed H-rotor Darrieus Vertical Axis Wind Turbine (VAWT) with cambered tubercle leading edge (TLE) blades", Energy, 175, pp. 278 - 291, (2019).
22. Mohamed M. H., "Performance investigation of H-rotor Darrieus turbine with new airfoil shapes", Energy, 47 (1), pp. 522 - 530, (2012).
23. Roy S. and Saha U., "Computational Study to Assess the Influence of Overlap Ratio on Static Torque Characteristics of a Vertical Axis Wind Turbine", Procedia Engineering, 51, pp. 694 - 702, (2013).
24. Sunny K. A., and Kumar N. M., "Vertical axis wind turbine: Aerodynamic modelling and its testing in wind tunnel." Procedia Computer Science 93: pp. 1017-1023, (2016).
25. Sharma A., and Murtaza M. A. "Modelling and Finite Element Analysis of Vertical Axis Wind Turbine Rotor Configurations", International Journal of Mechanical and Production Engineering Research and Development (IJMPERD) ISSN (P): pp. 2249-6890, (2016).
26. Wind Science: Betz limit, "Understanding Coefficient of Power (Cp) and Betz Limit", http://cdn.teachersource.com/downloads/lesson_pdf/betz_limit_0.pdf (access 30th May 2022)
27. Fanni M., Shabara M. N., and Alkalla M. G., "A Comparison between Different Topology Optimization Methods." MEJ. Mansoura Engineering Journal 38, No. 4: pp. 13-24, (2020).